

Influence of Nanostructured Zinc Titanate, Zinc Oxide or Titanium Dioxide Thin Film Coated on Fluorine Doped Tin Oxide as Working Electrodes for Dye-Sensitized Solar Cell

Mohammad Hossein Habibi^{1,*}, Maryam Mikhak¹, Mahmoud Zendeheel¹ and Mehdi Habibi²

¹ Nanotechnology Laboratory, Department of Chemistry, University of Isfahan, Isfahan, 81746-73441 I.R. Iran

² Department of Electrical Engineering, University of Isfahan, Isfahan, 81746-73441 I.R. Iran

*E-mail: habibi@chem.ui.ac.ir

Received: 6 July 2012 / Accepted: 19 July 2012 / Published: 1 August 2012

A series of working electrode metal oxide semiconductor nanostructured with zinc titanate, zinc oxide and titanium dioxide were coated on the fluorine-doped tin oxide (FTO) conducting glass as working electrodes in dye sensitized solar cells (DSSC). Zinc titanate (ZT), zinc oxide (ZO) and titanium dioxide (TD) nano-particles were synthesized by sol-gel method and characterized by scanning electron microscopy (SEM), X-ray diffraction (XRD) and UV-vis Diffuse reflectance spectrum (DRS). The influence of ZT, ZO and TD thin films was compared with standard titania cells, using D35 dye and an electrolyte containing [Co(bpy)₃](PF₆)₂, [Co(pby)₃](PF₆)₃, LiClO₄, and 4-tert-butylpyridine (TBP). Under the same working conditions, the properties of DSSC have been studied by measuring their short-circuit photocurrent density (J_{sc}), open-circuit voltage (V_{oc}) fill factor (ff) and conversion efficiency (η). The results showed that the cell made of the ZO particles exhibits the largest value of J_{sc} and V_{oc} among these three samples. The variation trend of V_{oc} is the same as that of J_{sc}, that is, ZO > ZT > ZD. The outcome of this study can be crucial for the preparation of reliable paste in a simple way for its application in DSSC.

Keywords: Working electrode; Zinc titanate; Zinc oxide; Nanoparticle; Dye-sensitized solar cell; Nanostructure

1. INTRODUCTION

Dye-sensitized solar cells (DSSC) have attracted much attention as low-cost alternatives to harvest solar energy since it was first reported in 1991 [1]. DSSC consists of a porous-structured nanocrystalline semiconductor coating electrode with adsorbed dye molecules as the photosensitized

anode, a platinized fluorine-doped tin oxide (FTO) glass as the counter electrode, and an electrolyte as a conductor to electrically connect the two electrodes [2-5]. Transition metal oxide semiconductor used as photoelectrode is sensitized by the injection of electron from the dye used as sensitizer in the cell. Layer of dye adsorbed in the nanoporous surface of semiconductor film absorbs light and goes to excited state where it injects electrons to the conduction band of semiconductor [6-8]. Compared to conventional silicon cells, the DSSC has lower power conversion efficiency [9-11]. A promising approach to enhance the conversion efficiency of a dye-sensitized solar cell is to decrease the recombination of electrons in the dye or electrolyte. An important aspect that determines cell performance is the kind of metal oxide semiconductor porous-structured coating electrode. The properties of porous coating electrode, such as surface area, roughness, pore size, and film thickness, which determine its surface and electronic properties, are mainly controlled by the film preparation process. DSSC based on zinc oxide-coated titania electrodes is reported using an expensive vacuum technology that required a sophisticated process control [12, 13].

In this study for the first time we have used three different metal oxide nano-particles such as zinc titanate (ZT), zinc oxide (ZO) and titanium dioxide (TD) and assemble DSSCs using them as the working photoelectrodes. A comparison of DSSCs with different working electrode with the conventional DSSC was reported.

2. EXPERIMENTAL

2.1 Preparation of materials

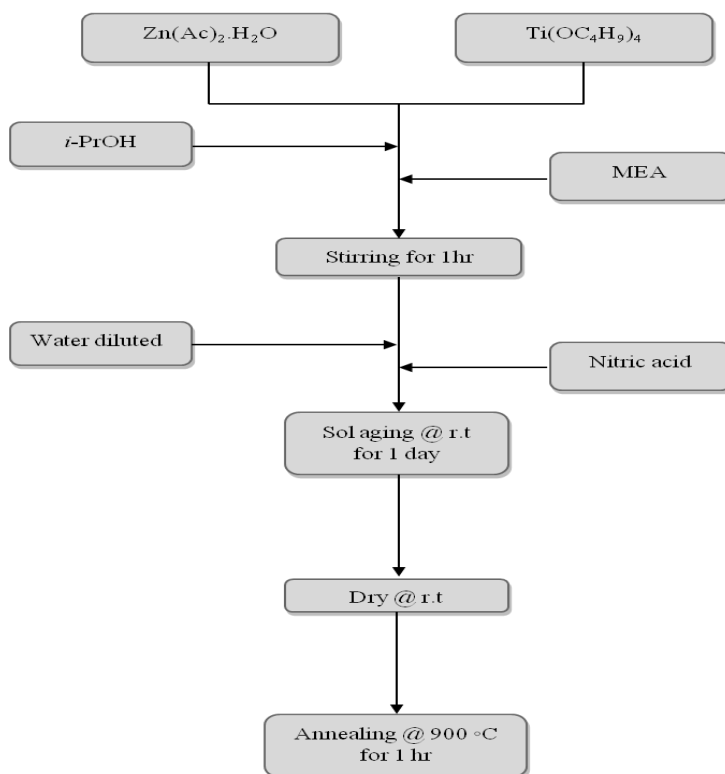


Figure 1. Flow chart for preparation of zinc titanate (ZT) nanoparticle

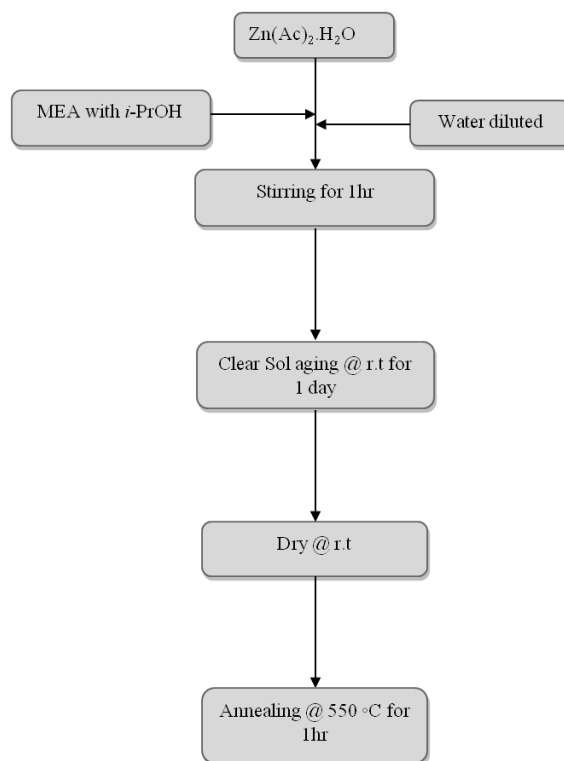


Figure 2. Flow chart for preparation of zinc oxide (ZO) nanoparticle

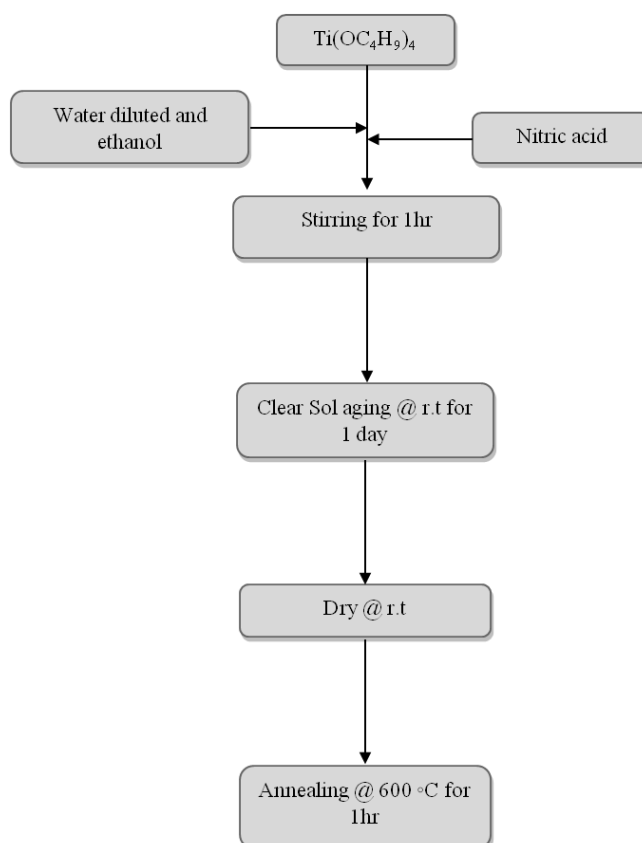


Figure 3. Flow chart for preparation of titania (TD) nanoparticle

Titanium tetraisopropoxide, zinc acetate and 1, 3-isopropanol analytical grade were used as titanium and zinc precursors, respectively. Nanostructure zinc oxide was prepared according to the following procedure: Zinc acetate dihydrate (14 mmol) and (14 mmol) monoethanolamine was dissolved in 15 mL isopropanol heated to 60 °C with continuous stirring for 60 minutes forming a clear solution (ZA sol). The ZA sol was preheated at 275 °C in air and annealed at 550 °C for 80 minutes [14-16]. For sol–gel preparation of nanostructure zinc titanate, ZnTiO₃, ZA sol was stirred and titanium tetraisopropoxide was added drop-wise forming a clear solution (ZT sol). The ZT sol were preheated at 110 °C for 1 h and annealed at 800 °C for 1 h (Figs 1-3) [17-19].

2.2. Assembling of working electrode.

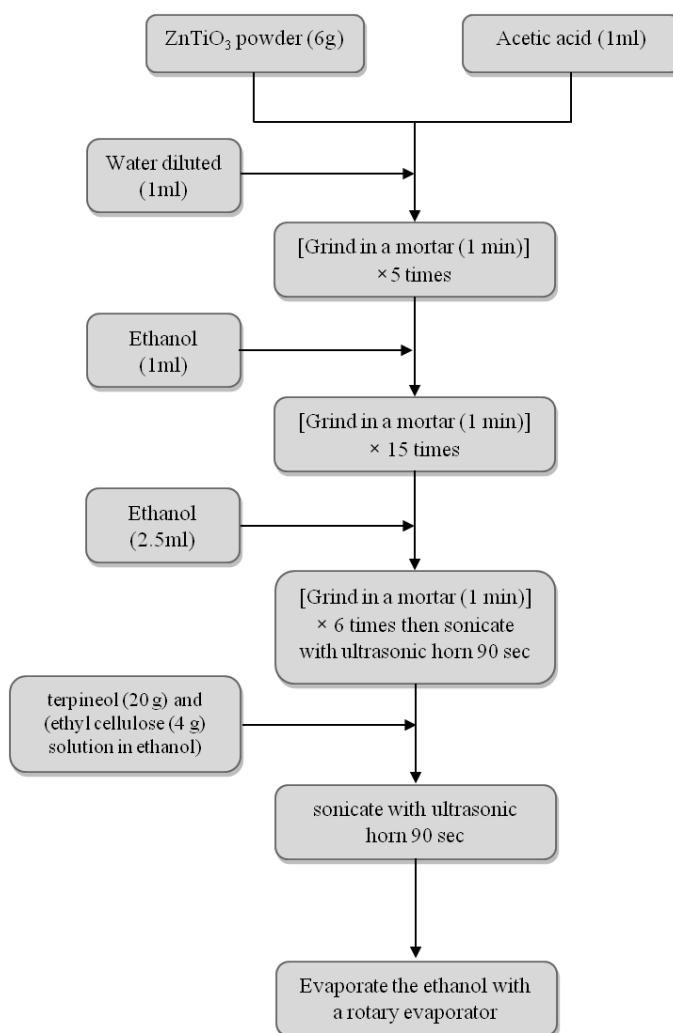


Figure 4. Flow chart for preparation of zinc titanate (ZT) paste for DSSC

Fluorine-doped tin oxide (FTO) glass substrates (Pilkington, TEC15) were cleaned in an ultrasonic bath overnight using (in order) detergent, water, and ethanol. The conducting glass substrates coated using spin coating method (Spin Coater, Modern Technology Development Institute,

Iran) with titanium sol and preheated in 105 °C for 10 min. Mesoporous TiO₂ films were prepared with an area of 0.12 cm² by doctor blade technique colloidal titania (TD), zinc oxide (ZO), ZnTiO₃ (ZT) paste (Fig. 4) and preheating at 120 °C and sintering. The temperature gradient program had four levels at 180 (10 min), 320 (10 min), 390 (10 min), and 500 °C (60 min).

2.3. Assembling of DSSCs

The working electrodes were immersed in a dye bath containing 0.2 mM D35 in ethanol and left 1 hr in 50 °C. The films were then rinsed in ethanol to remove excess dye. Solar cells were assembled, using a 30 μm thick thermoplastic Surlyn frame with a platinized counter electrode (TEC8) was prepared by depositing 10 μLcm⁻², 4.8 mM H₂PtCl₆ solution in ethanol to the glass substrate followed by heating in air at 400 °C for 30 min. An electrolyte solution was then introduced through two holes predrilled in the counter electrode, and the cell was sealed with thermoplastic Surlyn covers and a glass cover slip. Unless otherwise noted, the electrolyte consisted of 0.22 M [Co(bpy)₃](PF₆)₂, 0.033 M [Co(pby)₃](PF₆)₃, 0.1 M LiClO₄, and 0.2 M 4-tert-butylpyridine (TBP) in 3-methoxy propanitrile.

2.4. Characterization and Photoelectric Measurements

X-ray diffraction (XRD) patterns were recorded on a Bruker D8 advance X-Ray diffractometer. Morphology and film thickness were measured by Philips XL-30 scanning electron microscopy. Diffuse reflectance spectra were collected with a V-670, JASCO spectrophotometer and transformed to the absorption spectra according to the Kubelka-Munk relationship. Current-voltage characteristics of the DSSCs were measured by a HABSC12 I-V Testing Equipment for solar cell (Habibi Solar Photoelectric Technology). The devices under analysis were illuminated with a xenon lamp with AM1.5 equivalent (Lightdrive 1000, Fusion Lighting solar simulator, 1000Wm⁻² at 40 °C). The DSSCs were masked to expose only the active area under all measurements. Incident-light intensities were adjusted with light source distance. J-V curves were obtained by applying an external bias to the cell and measuring the generated photocurrent with a digital source meter. The voltage sweep range was 2V in a 20second period. The xenon lamp was used as the light source and its incident light intensity was measured by Radiation Meter (Habibi Solar Photoelectric Technology). Constructed solar cells were shielded by using a black metal mask with an aperture area of 0.25 cm² before the photovoltaic measurement. Current-Voltage (I-V) curves of the solar cells were characterized by using a Habibi-S source meter under illumination of simulated sunlight, which was provided by an Oriel solar simulator equipped with an AM1.5 filter. Electrochemical impedance spectroscopy measurements were performed by using a computer-controlled SAMA-500 in a frequency range of 0.005–105 Hz under 1 sun of AM1.5 solar radiation, and a bias corresponding to the open-circuit photovoltage, Voc, was applied. The amplitude of the alternating signal was 10 mV. ZView was then used to fit the impedance spectra by applying equivalent-circuit models of the DSC device.

3. RESULTS AND DISCUSSION

3.1. Characterization.

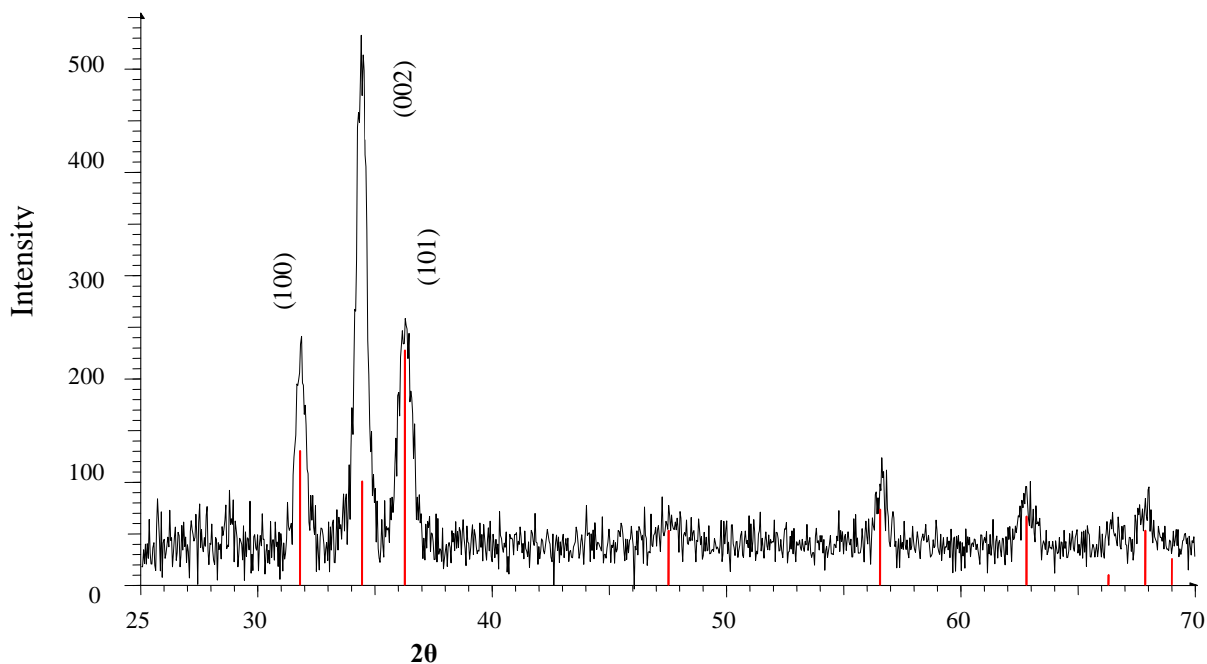


Figure 5. XRD patterns of zinc oxide (ZO) nanoparticle annealed at 500 °C

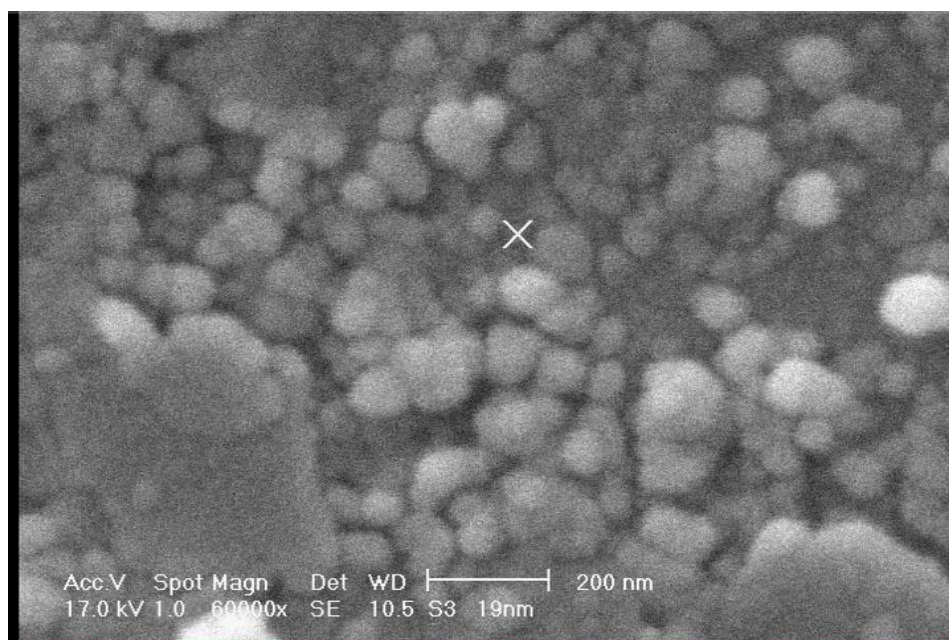


Figure 6. SEM image of ZT nanopowders derived by the sol-gel technique at 800 °C

Bragg's reflection for zinc oxide is observed in the XRD pattern (Fig. 5) [20-25]. Morphology of the ZT samples was obtained using SEM images [26-29]. Figure 6 shows the SEM images of the zinc titanate nanoparticles at 800 °C with their average size of a 19 nm (Fig. 6). The UV-vis DRS is

used to study the effect of calcination temperature on light absorption. The DRS of ZnTiO₃ samples annealed at 800 °C are shown in Fig. 7.

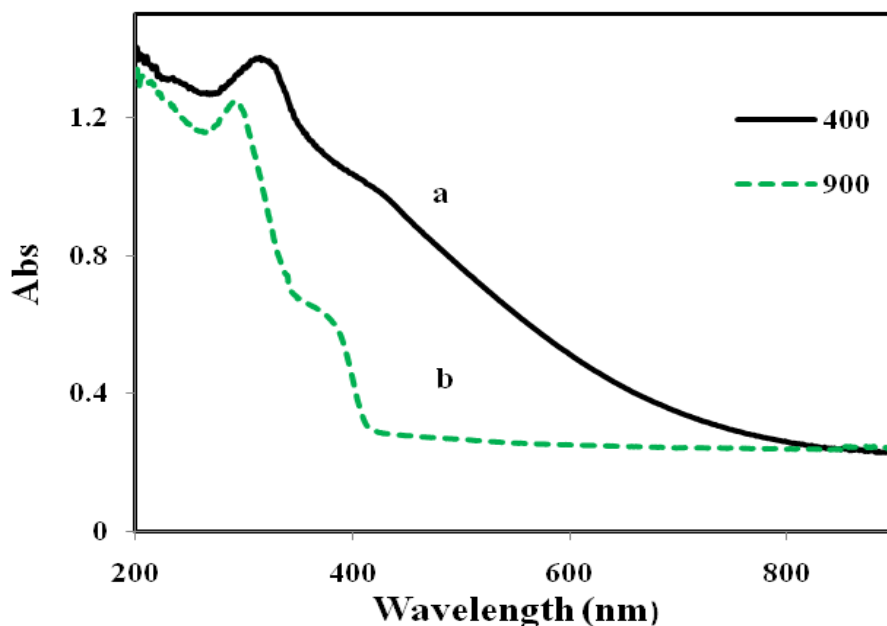


Figure 7. UV–vis diffuse reflectance spectra of ZnTiO₃

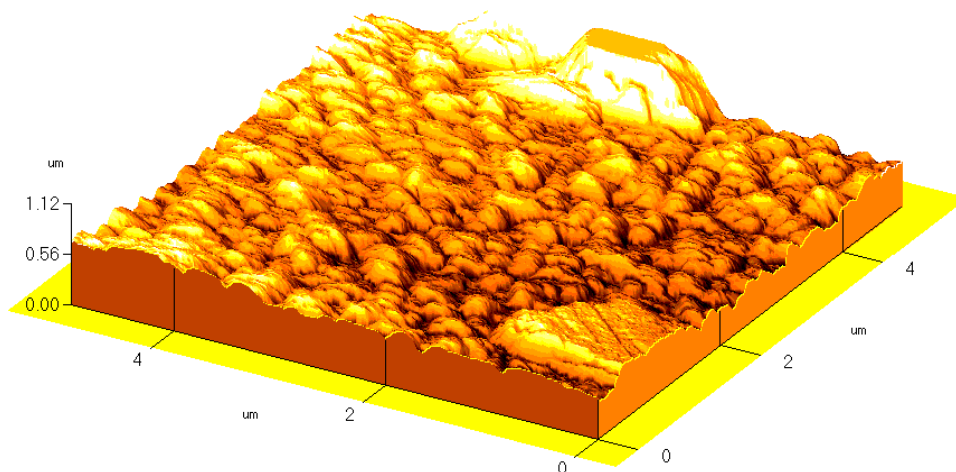


Figure 8. AFM images of surface morphology the titania thin film

The maximum absorbance appears at 296 nm for zinc titanate. A new absorption edge at higher wavelength (438 nm) for zinc titanate annealed at 900 °C is an indication that the nanopowder can absorb lights in the higher wavelength, and therefore they can more efficiently utilize light. AFM investigation of titania thin film showed that they are grain-like and results are consistent with SEM. The AFM micrograph of titania thin film is shown in Fig. 8.

3.2. Photovoltaic Performance of Cells.

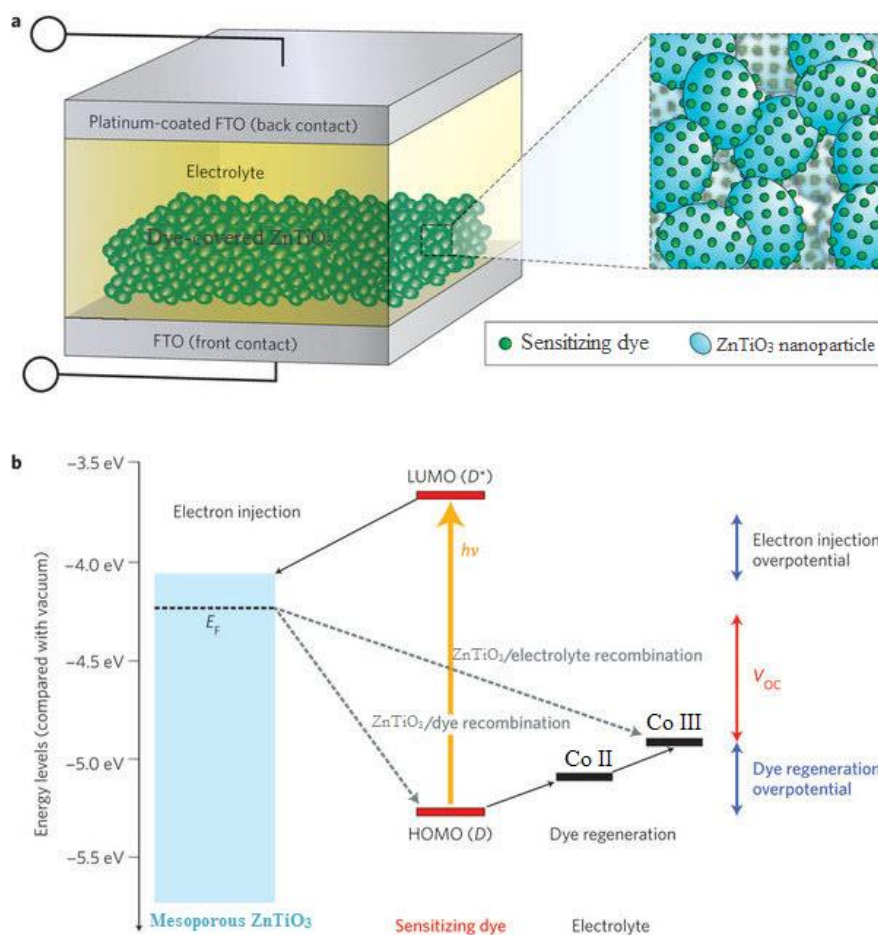


Figure 9. Schematic of (a) DSSC with a zinc titanate-coated titania electrode, (b) Schematic illustration of the electron flow in an operating DSSC

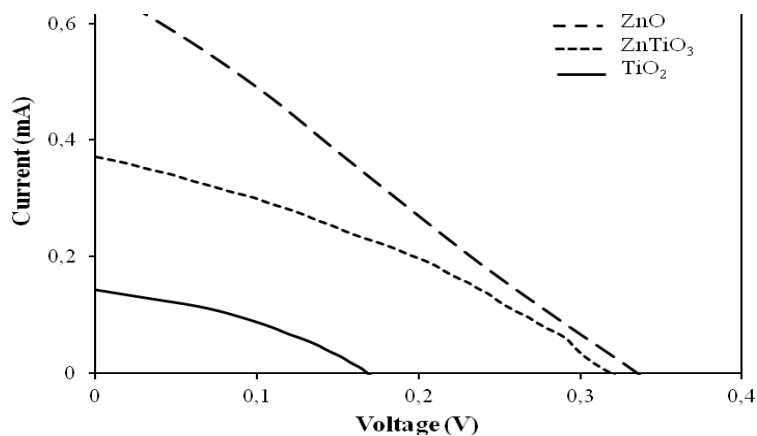


Figure 10. Current–voltage (I–V) characteristics of dye sensitized solar cells (DSSC) prepared by zinc oxide (ZO), titania (TD) and zinc titanate (ZT) nano-particles with FTO titania film at one sun illumination (1000mWm^{-2} , AM 1.5).

The three dye sensitized electrodes were used as the working electrodes in sandwich solar cells (Fig. 9). Figure 10 the I-V characteristics for 0.12 cm^2 open cell under the light irradiation of 1000 mWm^{-2} (measured by Radiation Meter). All the samples exhibit a typical behavior of the I-V curve for DSSCs. The open-circuit voltage V_{OC} and the short-circuit current density J_{SC} for the ZO, ZT, and TD are 340 mV and 6.0 mA cm^{-2} , 320 mV and 4.0 mA cm^{-2} , 170 mV and 1.40 mA cm^{-2} , respectively. The fill factor ff , which is defined as $P_{max}/(V_{OC} J_{SC})$, where P_{max} is the maximum power output, for the TD, ZT, and ZO samples are calculated to be 72%, 62%, and 56%, respectively [30-37]. The energy conversion efficiency is $ZO > ZT > ZD$ and the cell made of the ZO particles exhibits the largest value of J_{SC} and V_{OC} among these three samples.

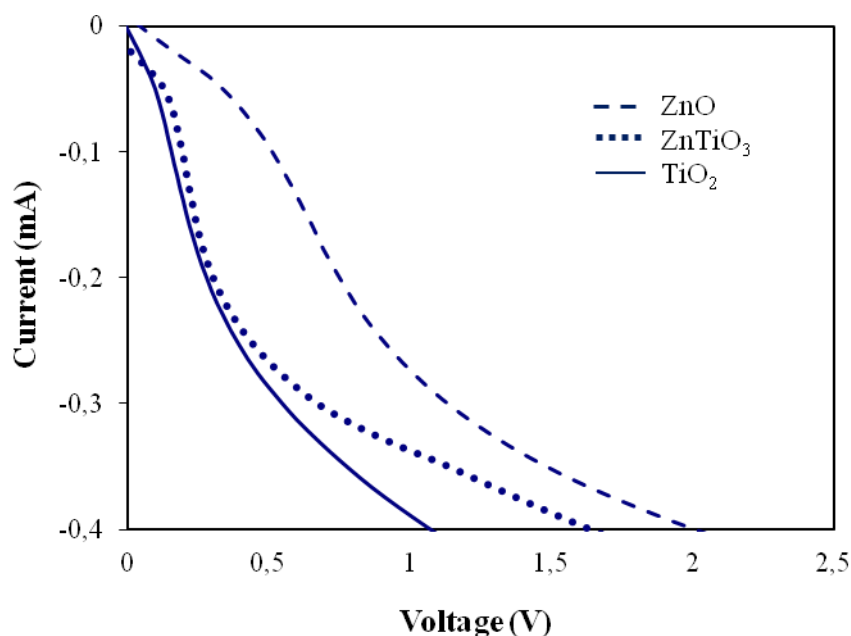


Figure 11. Dark current–voltage (I–V) characteristics of dye sensitized solar cells (DSSC) prepared by zinc oxide (ZO), titania (TD) and zinc titanate (ZT) nano-particles with FTO titania film.

The variation trend of V_{OC} is the same as that of J_{SC} , that is, $ZO > ZT > ZD$. The difference of cell properties for the different metal oxide particles might be related to the amounts of adsorbed dye on the three electrodes [38-41]. The improvement of the performance of DSCs can be related to the ZO electrodes which have the benefit to the dye adsorption, light absorption and the electrolyte transportation [42-44]. Figure 11 shows the dark current–voltage characteristics of the three kinds of dye sensitized solar cells (DSSC) prepared by ZO, TD and zinc titanate (ZT) nano-particles with FTO titania film with dye. The onset of the dark current of TD occurred at low forward bias. Using a zinc titanate under-layer suppresses the dark current, shifting its onset. This indicates that the cobalt complex reduction at the exposed part of FTO is responsible for the high dark current observed with the nanocrystalline titania film [45-47]. Zinc titanate and zinc oxide on underlayered films shifted the I–V curves to slightly lower voltages. This is attributed to increasing the electron trap site on the titania surface with enlarging the surface area by zinc titanate and zinc oxide. On the other hand, the dark-

current curves of DSSC prepared by ZO and ZT nano-particles with FTO titania film with dye were shifted to slightly lower voltages indicating that the sensitizer increases the dark current on electrodes where the FTO surface is already blocked [48]. This is attributed to titania band shifting to positive values by surface protonation. In a typical open-circuit voltage decay (OCVD) measurement, the light is switched off, and the voltage decay under open-circuit conditions and in the dark are monitored. In this case no electrons are injected into the film apart from those already present and the diffusion term is zero because no macroscopic gradient is sustained within the oxide film at open-circuit. Solar cell electron decay for three kinds of dye sensitized solar cells (DSSC) prepared by ZO, TD and zinc titanate (ZT) nano-particles with FTO titania film with dye was measured by monitoring transient photocurrent decay which shows typical exponential behavior.

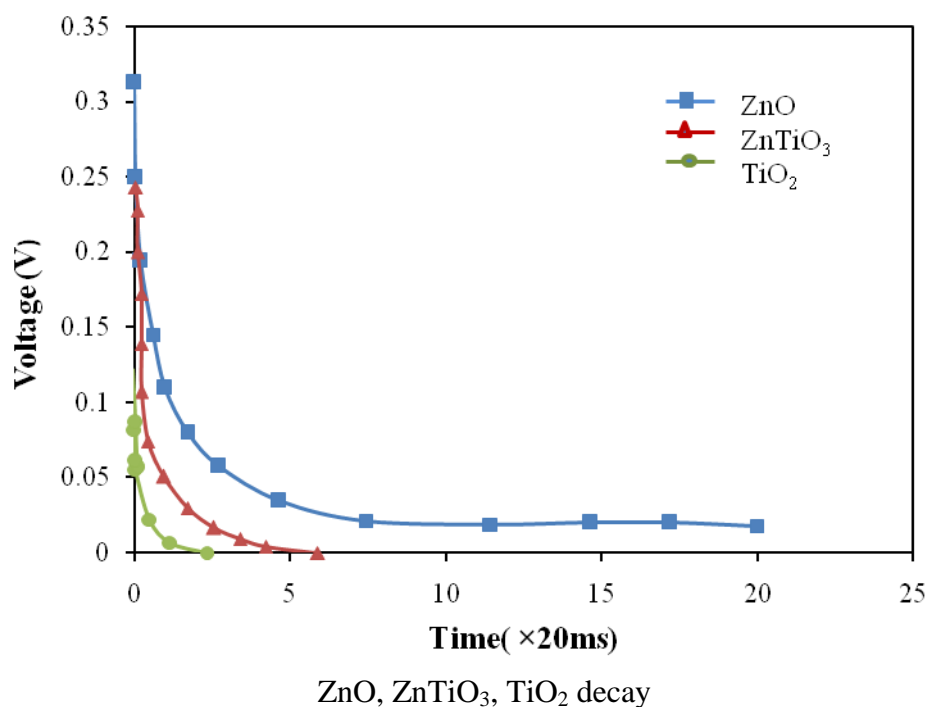


Figure 12. Experimental Voc decay results of dye sensitized solar cells (DSSC) prepared by zinc oxide (ZO), titania (TD) and zinc titanate (ZT) nano-particles with FTO titania film.

Figure 12 shows open-circuit voltage-decay curves for the three DSSC prepared by ZO, TD and ZT nano-particles with FTO titania film after the illumination was turned off [49-51]. The response time increases with decreasing Voc. It can be seen that the response time of is the same as that of JSC, that is, $ZO > ZT > TD$. The insight into the enhancement in performance can be obtained by investigating the photoelectron lifetimes using the open-circuit voltage-decay measurements.

4. CONCLUSION

In summary, a series of metal oxide porous film electrodes were prepared by doctor blade technique using sol-gel method and the corresponding dye-sensitized solar cells were made. Effects of

metal oxide on the photovoltaics of the DSCs were studied. The results showed that variation trend $ZD < ZT < ZO$ is observed for short-circuit photocurrent density (J_{sc}) and open-circuit voltage (V_{oc}) resulting in enhancing the conversion efficiency. These enhancements were attributed to the high electron conductivity of ZnO, the improved dye adsorption and high light transmittance of composite film. The cell made up of the ZO particles shows the best photovoltaic performance among these three cells. Based on the analysis of the dye loading and surface photovoltage spectroscopy for the dye-sensitized electrode materials, the best performance is probably due to the highest loading amount of dye and best interaction between the semiconductor and dye.

ACKNOWLEDGEMENTS

The authors wish to thank the University of Isfahan for financially supporting this work.

References

1. B. O'Regan, M. Grätzel, *Nature*, 353 (1991) 737.
2. F.T. Kong, S.Y. Dai, K.J. Wang, *Adv. Optoelectron.* 7 (2007) 75384.
3. T-H. Tsai, Sh-Ch. Chiou, Sh-M. Chen, *Int. J. Electrochem. Sci.* 6 (2011) 3333.
4. L. Y. Lin, C. P. Lee, R. Vittal and K. C. Ho, *J. Power Sources.* 196 (2011) 1671.
5. Z. Wei, Y. Yao, T. Huang and A. Yu, *Int. J. Electrochem. Sci.* 6 (2011) 1871.
6. S. K. Dhungel, J. G. Park, *Renewable Energy.* 35 (2010) 2776.
7. M. Grätzel, *Chemistry Letters.* 34 (2005) 8.
8. U. O. Krasovec, M. Berginc, M. Hocevar, M. Topic, *Solar Energy Materials & Solar Cells.* 93 (2009) 379.
9. C.S. Chou, R.Y. Yang, M.H. Weng, C.H. Yeh, *Powder Technology.* 187 (2008) 181.
10. C.S. Chou, R.Y. Yang, C.K. Yeh, Y.J. Lin, *Powder Technology.* 194 (2009) 95.
11. C.S. Chou, R.Y. Yang, C.K. Yeh, Y.J. Lin., K.H. Liu, *Advanced Powder Technology.* 22 (2011) 31.
12. S. Wu, H. Han, Q. Tai, J. Zhang, B.L. Chen, S. Xu, C. Zhou, Y. Yang, H. Hu, X.Z. Zhao, *Applied Physics Letters.* 92 (2008) 122106.
13. Y. Jiang, Y. Yan, W. Zhang, L. Ni, Y. Sun, H. Yin, *Applied Surface Science.* 257 (2011) 6583.
14. M.H. Habibi, M. Khaledi Sardashti, *J Adv Oxid Technol.* 12 (2009) 231.
15. M.H. Habibi, M. Khaledi Sardashti, *J Iran Chem Soc.* 5 (2008) 603.
16. M.H. Habibi, M. Khaledi Sardashti, *Z Naturforsch.* 63a (2008) 440 .
17. M.H. Habibi, M. Mikhak, *Curr. Nanosci.* 7 (2011) 603.
18. M.H. Habibi, M. Mikhak, *Appl Surf Sci.* 258 (2012) 6745.
19. M.H. Habibi, M. Mikhak, *J. Adv. Oxid. Technol.* 15 (2012) 348.
20. MR. Mohammadia, D. J. Fray, *Journal of the European Ceramic Society.* 30 (2010) 947.
21. C. Zongying, L. Junshou, W. Yigang, *Journal of Alloys and Compounds.* 489 (2010) 167.
22. L. Wang, H. Kang, D. Xue, C. Liu, *J. Cryst. Growth.* 311 (2009) 611.
23. Z. Liu, D. Zhou, S. Gong, H. Li, *J. Alloy Compd.* 475 (2009) 840.
24. A. Chaouchi, S. d'Astorg, S. Marinel, M. Aliouat, *Mater Chem Phys.* 103 (2007) 106.
25. YS. Chang, YH. Chang, IG. Chen, GJ. Chen, YL. Chai, T.H. Fang, *Ceram Int.* 30 (2004) 2183.
26. YS. Chang, YH. Chang, IG. Chen, GJ. Chen, YL. Chai, *J Cryst Growth.* 243 (2002) 319.
27. YS. Chang, YH. Chang, IG. Chen, GJ. Chen, YL. Chai, T.H. Fang, S. Wu *Ceram Int.* 30 (2004) 2183.
28. L. Zhao, F. Liu, X. Wang, Z. Zhang, J. Yan, *J Sol-Gel Sci Technol.* 33 (2005) 103.

29. L. Wang, H. Kang, D. Xue, C. Liu, *J Cryst Growth*. 311 (2009) 611.
30. S. K. Dhungel, J. G. Park, *Renewable Energy*. 35 (2010) 2776.
31. Fu-an. Guo, G. Li, W. Zhang, *Journal of Photoenergy*. 1155 (2010) 105878
32. A. Hagfeldt, G. Boschloo, L. Sun, L. Kloo, H. Pettersson, *Chem. Rev.* 110 (2010) 6595.
33. J. H. Yum, D. P. Hagberg, S. J. Moon, K. M. Karlsson, T. Marinado, L. C. Sun, A. Hagfeldt, M. K. Nazeeruddin, M. Gratzel, *Angew. Chem., Int. Ed.* 48 (2009) 1576.
34. A. Hagfeldt, N. Vlachopoulos, M. Graätzel, *J. Electrochem. Soc.* 141 (1994) L82.
35. C. Bauer, G. Boschloo, E. Mukhtar, A. Hagfeldt, *Chem. Phys. Lett.* 387 (2004) 176.
36. G. Boschloo, A. Hagfeldt, *J. Phys. Chem. B.* 105 (2001) 3039.
37. G. Boschloo, L. Haäggman, A. Hagfeldt, *J. Phys. Chem. B.* 110 (2006) 13144.
38. T. Privalov, G. Boschloo, A. Hagfeldt, P. H. Svensson, L. Kloo, *J. Phys. Chem. C.* 113 (2009) 783.
39. M. Quintana, T. Marinado, K. Nonomura, G. Boschloo, A. Hagfeldt, *J. Photochem. Photobiol., A* 202 (2009) 159.
40. Y. Hao, X. Yang, J. Cong, H. Tian, A. Hagfeldt, L. Sun, *Chem. Commun.* 27 (2009) 4031.
41. D. P. Hagberg, J. H. Yum, H. Lee, F. De Angelis, T. Marinado, K. M. Karlsson, R. Humphry-Baker, L. C. Sun, A. Hagfeldt, M. Graätzel, M. K. Nazeeruddin, *J. Am. Chem. Soc.* 130 (2008) 6259.
42. J. H. Yum, D. P. Hagberg, S. J. Moon, K. M. Karlsson, T. Marinado, L. C. Sun, A. Hagfeldt, M. K. Nazeeruddin, M. Gratzel, *Angew. Chem., Int. Ed.* 48 (2009) 1576.
43. J. Wiberg, T. Marinado, D. P. Hagberg, L. C. Sun, A. Hagfeldt, B. Albinsson, *J. Phys. Chem. C.* 113 (2009) 3881.
44. H. N. Tian, X. C. Yang, R. K. Chen, A. Hagfeldt, L. C. Sun, *Energy EnViron. Sci.* 2 (2009) 674.
45. A. Morandeira, G. Boschloo, A. Hagfeldt, L. Hammarstrom, *J. Phys. Chem. C.* 112 (2008) 9530.
46. P. Qin, M. Linder, T. Brinck, G. Boschloo, A. Hagfeldt, L. Sun, *Adv. Mater.* 21 (2009) 2993.
47. U. B. Cappel, E. A. Gibson, A. Hagfeldt, G. Boschloo, *J. Phys. Chem. C.* 113 (2009) 6275.
48. H. N. Tian, X. C. Yang, R. K. Chen, R. Zhang, A. Hagfeldt, L. C. Sun, *J. Phys. Chem. C.* 112 (2008) 11023.
49. J. Villanueva, J. A. Anta, E. Guille'n, G. Oskam *J. Phys. Chem. C.* 113 (2009) 19722.
50. M. H Habibi, M. Zendejdel, *Curr Nanosci.* 6 (2010) 642.
51. M. H Habibi, M. Nasr-Esfahani, G. Emtiazi, B. Hosseinkhani, *Curr Nanosci.* 6 (2010) 324.